Journal Name

ARTICLE

Fully spray-coated organic solar cells on woven polyester cotton fabric for wearable energy harvesting applications

Received 00th January 20xx,
Accepted 00th January 20xx

DOI: 10.1039/x0xx00000x

www.rsc.org/

S. Arumugam,*[a] Y. Li,[a] S. Senthilarasu,[b] R. Torah,[a] A.L. Kanibolotsky,[c] A.R. Inigo,[c] P.J. Skabara[c] and S.P. Beeby[a]

This paper presents the novel use of spray-coating to fabricate organic solar cells on fabrics for wearable energy harvesting applications. The surface roughness of standard woven 65/35 polyester cotton fabric used in this work is of the order of 150 µm and this is reduced to few microns by a screen printed interface layer. This pre-treated fabric substrate with reduced surface roughness was used as the target substrate for the spray-coated fabric organic solar cells that contains multiple layers of electrodes and active materials. A fully spray-coated photovoltaic (PV) devices fabricated on fabric substrates has been successfully demonstrated with comparable power conversion efficiency to the glass based counterparts. All PV devices are characterised under simulated AM 1.5 conditions. Device morphologies were examined by scanning electron microscopy (SEM) and atomic force microscopy (AFM). This approach is potentially suitable for the low cost integration of PV devices into clothing and other decorative textiles.

Introduction

This paper concerns the development of organic solar cells on flexible fabric substrates. The fabric substrate places many constraints on the fabrication of the devices, which means existing processes, and technologies cannot be simply applied directly onto the textile. The first generation solar cells based on silicon are the market leader in the PV industry.[1] However, these first generation cells are rigid, costly and consume high levels of energy in production and are not compatible with textiles. The second generation of thin film based copper indium gallium selenide (CIGS), cadmium tellurium (CdTe) solar cells are attracting more attention due to reduced materials usage, low cost preparation techniques and broad solar coverage, compared to first generation devices. These solar cells have already reached 20% efficiency on rigid substrates.[1, 2] However, the fabrication of second generation solar cells still involves high temperature treatments and vacuum processes which are incompatible with textile substrates. In addition, there is a growing concern about toxicity and after life disposal, which is a barrier to commercialisation. Third generation solar cells are based on solution processed organic materials that are used to fabricate dye-sensitised solar cells (DSSCs), perovskite solar cells and polymer based organic solar cells (OSCs).[3-5] The low cost preparation techniques are making third generation solar cells more attractive in flexible solar cell applications with excellent potential for large area power generation. In particular, there is considerable ongoing research in OSCs towards improving device efficiency and fabrication processes.[6-8] These processes and materials do have the potential for the realisation of solar cells on fabric substrates. In recent years, wearable technologies derived from e-textiles have been developed for various applications, for example, medical, sports and military clothing.[9-12] The topic of energy harvesting is concerned with the conversion of ambient energy (e.g. kinetic, thermal or light) into electrical energy for use in powering autonomous systems. There is naturally considerable interest in using energy harvesting in wearable applications, which can extend the life, or potentially replace standard battery based power supplies. Fabric solar cells are one form of energy harvesting that has great potential for powering wearable devices. However, incorporating solar cells on fabric substrates is not straightforward. Fabrics are highly flexible substrates with different mechanical structures depending upon, for example, the weave and yarn parameters. The surface of a fabric is rough compared to a plastic substrate such as polyimide film (Kapton, trade name of Dupont) and their use will limit the maximum temperature that can be used in device processing.

Existing examples of solar cells on fabrics use conventional rigid silicon or plastic solar cells, as standalone PV devices, which are attached (stitched or glued) onto the fabric as a functional patch.[13] This approach makes the fabric relatively inflexible and alters the feel of the textile dramatically and the fabric itself has no added functionality. However, a new generation of flexible DSSCs and OSCs offer the potential for integrating the light harvesting capability into the fabric itself providing a low weight

[a] Printed Electronics and Materials laboratory, Electronics and computer science, University of Southampton, UK, SO17 1BJ. E-mail: S.Arumugam@soton.ac.uk
[b] Environment and Sustainability Institute, University of Exeter, Cornwall, TR10 9FE.
[c] WestCHEM, Department of Pure and Applied Chemistry, University of Strathclyde, Glasgow, UK, G1 1XL.
Electronic Supplementary Information (ESI) available: See DOI: 10.1039/x0xx00000x

solution that maintains the feel of the fabric. Integrating DSSCs and OSCs on fabric substrates has many challenges, such as achieving suitable device flexibility and durability, acceptable conversion efficiency and fabrication using processes compatible with the textile industry.

Research in the fabrication of flexible solar cells integrated into fabrics has explored several approaches, especially using organic polymer materials for DSSCs and OSCs. Recently, there are many published results on yarn based textile DSSCs,[14-25] have been woven into textiles. At the same time research studies show the bending cycles will significantly disable or degrade the PV yarns performance.[19, 21, 23] In the conventional DSSCs architecture, there are two fluorine tin oxide (FTO) coated glass substrates sandwiched together with the introduction of liquid electrolyte in between them. Approaches to the fabric DSSCs has replaced one of the two FTO coated glass slides to the conductive fabrics, for example, carbon nanotube coated fabrics,[26] nickel coated woven polyester fabric[27] and graphene coated cotton fabrics.[28] However, the fully sprayed DSSCs on fabrics for wearable applications has never been demonstrated, as they used the coated fabrics as a stick-on electrode to the FTO glass substrate, which are not flexible, nor wearable. Fabric OSCs were fabricated using a combination of evaporation and spin-coating by Bedeloglu *et al.*[29-32] This work actually used a non-woven polypropylene textile tape as the substrate which is not representative of typical woven fabrics. These devices did work and achieved 0.2% efficiency, which is the highest value reported to date from a coated organic PV textile. Krebs *et al.*[33] used a standard woven textile and smoothed the surface by laminating a polyethylene film for OSCs. This film has a low surface energy and requires a plasma treatment to enable subsequent films to be deposited. These films were deposited by a combination of screen printing and evaporation and did not function due to short circuiting. Another approach by Lee *et al.*[34] fabricated OSCs on a flexible PET/ITO substrate, which was then attached to a conductive fabric which acted as the bottom electrode. This approach does not add functionality to the textile itself and uses evaporation processes for some of the films. Other research has explored fabricating a functional organic PV fibre which can then be woven into a textile.[35-38] This approach demonstrated a maximum efficiency of 0.5%, but the method fundamentally limits the output of the solar cell because once woven into a textile the PV layer is inevitably partially shaded. This approach is also being explored in the European Union funded project Powerweave[39] but this has yet to report any results on fibres. Inorganic solar cells on fabrics has only been reported once in literature, the evaporated CIGS PV textiles have been demonstrated by Powertextile Ltd with a reported efficiency of 13%.[40] This is a promising value for harvesting energy but the evaporation based fabrication method isn't compatible with large scale textile manufacture and the material toxicity remains a significant concern.

Whilst the organic functional layers in OSCs are deposited using solution-based processes such as spin-coating, spray-coating, precision-die coating, inkjet printing and dip-coating, the cathode and anode metal layers have typically been deposited using vacuum based thermal evaporation.[41-45] This was due to the absence of a suitable solution based process for electrodes that give a low work function. Recently, however, several research groups have evaluated silver nanowire (AgNW) solutions for use as flexible electrodes to fabricate OSCs. These have demonstrated a comparable power conversion efficiency (PCE) to those using indium tin oxide (ITO) and other metal evaporated electrodes.[46-49] Most recently, Guo *et al.* reported solar cells on glass substrates fabricated entirely by solution based processing with AgNW as top and bottom electrodes.[50, 51] However, a detailed study of an entirely solution processed device on a fabric substrate has not yet been demonstrated. Moreover, fully spray-coated OSCs on standard woven polyester cotton fabric have never been reported.

Among the various solution process techniques, spray-coating can accept a much wider range of rheological dispersions or solutions compared to inkjet printing, which has a strict acceptance range of the functional ink's rheological properties. The principle of spray-coating is to atomise the dispersion or solution, therefore enabling thin films to be deposited which is essential to achieve functional OSCs. Other solution based processes such as spin-coating are not compatible with large scale textile manufacture and dip-coating techniques would consume large quantities of active material due to the porous nature of the fabric. In this work, we have produced fabric based solar cells using a fully spray-coated method to obtain functional photovoltaic textiles that are processed in low temperature conditions (<150 °C) on a standard 65/35 polyester cotton fabric.

Experimental methods

The approach described in detail below involves using a screen printable polyurethane based interface paste (Fabink-UV-IF1) to smooth the fabric surface and this is available from Smart FabricInks Ltd. The standard 65/35 polyester cotton fabric was supplied by Klopman International. Metallic AgNW suspension in isopropyl alcohol (IPA), supplied by Nanopyxis, was used as the electron and hole collecting electrodes. Thin electron transport layer of ZnO-NP with average particle size <35nm dispersion (40 wt%) in ethanol was supplied by Buhler. The hole transport layer poly(3,4-ethylenedioxythiophene) polystyrene sulfonate (PEDOT:PSS) dispersion in water was supplied by Heraeus (PH1000). A blend of poly (3-hexylthiophene) (P3HT): indene-C_{60} bisadduct (ICBA), dissolved in 1, 2 dichlorobenzene were supplied by Plextronics was used as the photoactive layer. Kintec supplied patterned ITO glass substrates. These materials were used as supplied with no further modifications being required in order to use them in the spray coating process. Transmittance measurements were examined using Bentham PV instrumentation.

Fabrication of OSCs by spray-coating method

The construction of fabric solar cells begins by screen printing an interface layer onto fabric substrates. The purpose of the interface layer is to reduce the surface roughness of the fabric and present a smooth layer to support the subsequent spray-coated films. The screen design ensures that the interface layer is only printed where required, thereby maintaining the fabric's flexibility and maximising breathability compared to commercial pre-coated fabrics. The printer squeegee pressure setting was set to 6 kg and the printing gap was 0.8 to 1 mm. The film is cured with a UV dose of 1500 mJ/cm^2 thereby avoiding a thermal curing process that would release potentially harmful volatile organic compounds. The interface layer has a surface free energy of ~35 mN/m which was measured using a Kruss DSA30B tensiometer. This value confirms that the surface promotes the wettability of the majority of solvent based functional electronic inks, which have a lower surface tension typically around 30 mN/m. The ink's wettability, representing the interaction between ink and substrate, defines the pattern definition before the curing stage. The interface layer coated fabric substrate (IF fabric) has good thermal resistance and can withstand processing temperatures of 150 °C for up to 45 minutes in a conventional thermal oven without degradation. This is important since it constrains the materials and processes used in subsequent film depositions. The 65/35 polyester cotton fabric is a commonly used textile for standard clothing.

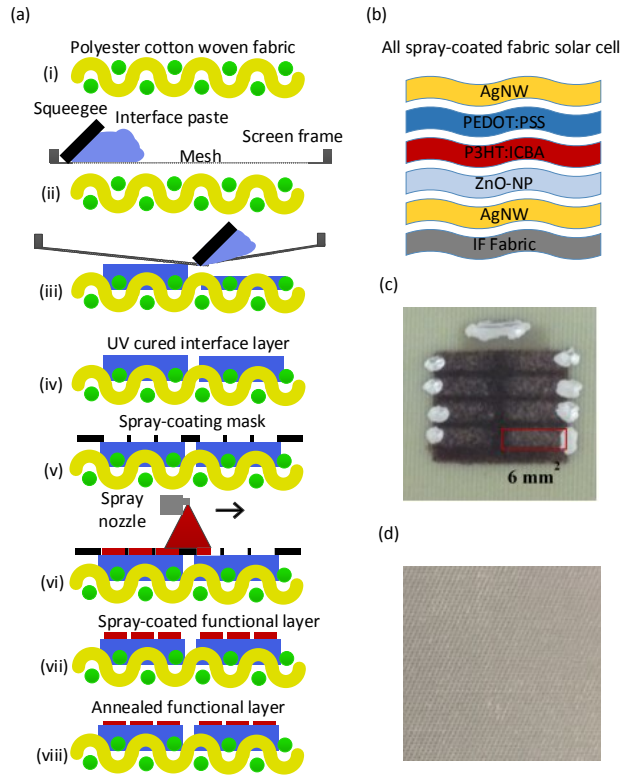

Fig. 1 (a) Cross-sectional view of the fabrication process of spray-coated fabric solar cells, (b) device structure of a fully solution-processed spray-coated fabric substrate, (c) The plan view of an optimised fabric solar cells, (d) The plan rear view of fabric solar cells.

Figure 1(a) shows a cross-section of the fabrication process, comprising two deposition stages for the interface and one functional layer. Figure 1 (i) – (iv) shows the screen printing of the interface layer on the fabric substrate. As there are typically five functional layers in the solar cell structure, stage (v) to (viii) were repeated 4 more times after the first functional layer deposition to obtain the multilayer spray-coated fabric solar cells shown in figure 1b. Figure 1 (c) shows the plan view of the spray coated solar cells on fabrics with 8 pixels being fabricated in one device. Figure 1(d) shows the plan rear view of the solar cells fabric substrate, which demonstrates the addition of the interface and the spray coated solar cells, does not change the feel and appearance of the underside of the fabric. The first functional layer of fabric solar cells is the bottom electrode, comprising the AgNW, as it has better flexibility than evaporation of thin metal layers in which micro cracks can occur while bending.[52] The spray-coating distance was initially 15 cm from the spray nozzle to the substrate with a differential pressure inlet/outlet of 0.3 bar. All spray-coating steps were performed under ambient atmospheric conditions. For the preliminary experiment the coating parameters remained the same for the deposition of all the functional layers on the IF fabrics. However, the devices made in the optimised stage has an increased spraying distance to obtain the reduced layer thickness. The spray distance became 20 cm for AgNW, P3HT:ICBA and PEDOT:PSS layers while maintaining 30 cm for ZnO-NP layer. The spray-coated AgNW layer was baked at 130 °C for 5 minutes in a box oven to obtain an AgNW film with thickness of ~100 nm. The ZnO-NP dispersion was successively spray-coated on top of the AgNW bottom electrodes and baked at 60°C for 10 minutes to obtain a solidified layer. Afterwards, the PV layer of P3HT: ICBA was spray-coated onto the top of the ZnO-NP layer. The deposited layers were subsequently annealed in an argon oven at room temperature, ramping up to 135 °C in 30 minutes, then annealed for a further 30 minutes. Then, the hole transport layer PEDOT:PSS was spray-coated and baked at 100 °C in a box oven for 5 minutes. To complete the device fabrication, a semi-transparent AgNW electrode was spray-coated on top of the PEDOT:PSS layer.

During processing, the fabric substrates were glued to an alumina tile that supported the fabric keeping it flat for each subsequent functional layer deposition. The performance of the fabric solar cells was tested after peeling off from the alumina tiles. The peeling off angle to the alumina tile is about 60 degree. In addition, pre-heating the alumina tile under 50 °C on a hotplate facilitated the peeling-off process, minimising potential damage that might be caused by the strain. The standalone fabric solar cells showed good flexibility after peeling off. For the purposes of comparison, we also fabricated the OSCs by spray-coating onto glass substrates using the same parameters. In addition, we also fabricated fabric solar cells utilising a spin-coating and evaporation method. Experimental and fabrication details of the spin-coated fabric solar cells are given in the supporting information. There were 48 devices made for each device type and all spray-coated devices were measured in ambient atmosphere immediately after fabrication. However, we only report the best performing cell in

terms of conversion efficiency for each device type. The measurement results of the other devices show relative low conversion efficiencies of 1 to 2 orders of magnitude lower, comparing to the best performance device. Differences are due to inconsistent processing and uneven film coverage. The current density versus voltage (J/V) curves of photovoltaic devices were obtained by a Keithley 2400 source meter unit. The photocurrent was measured under AM 1.5 (100mW/cm^2) irradiation using an ABET solar simulator, calibrated with a standard Si solar cell. The effective area of each cell is 6mm^2 and was defined by the shadow mask. The surface morphology of the AgNW was examined by field emission scanning electron microscopy (FESEM) analysis using a JEOL JSM 7500F instrument. The cross-section of the fabric solar cells was examined by an EVO Zeiss SEM. Tapping mode atomic force microscopic (AFM) measurements have been carried out to evaluate the surface morphology on each function layers using Veeco Innova instruments.

Results and discussion

Figure 2(a) shows a cross-sectional view of the woven 65/35 polyester cotton fabric structure with interlacing warp and weft yarns, which illustrates the rough surface profile of the material. Figure 2(b) shows a cross-sectional view of the fabric after printing of the interface layer with three layers being required to obtain a smooth interface surface with an average thickness of 150 µm. Figure 2 (c) presents an SEM image of an AgNW electrode viewed from above on a fabric substrate using the spray-coating method. The nature of the randomly dispersed AgNW forms overlapping wires each a few tens of micrometres in length and a few tens of nanometres in diameter. As shown in figure 2 (d), subsequent deposition of the ZnO-NP layer reduces the surface roughness of the AgNW due to the ZnO-NP filling up the scaffold structure of the AgNW.

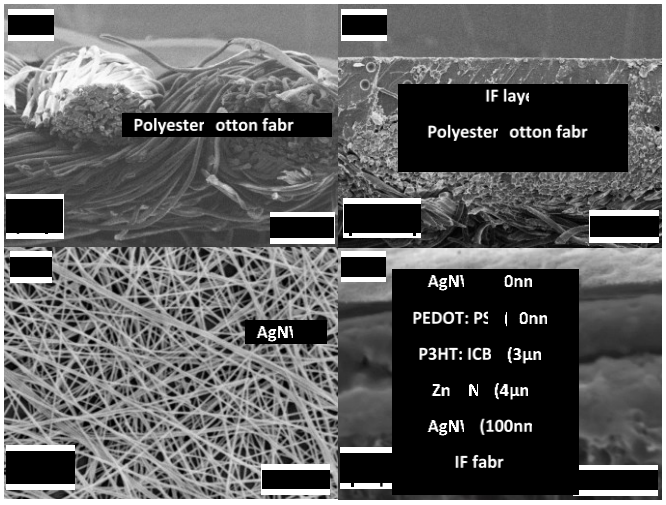

Fig. 2 (a) Cross-sectional view of woven 65/35 polyester cotton fabric substrate, (b) IF fabric substrate, (c) FE-SEM image of spray-coated bottom AgNW electrodes on a fabric substrate, (d) cross-sectional SEM image shows the spray-coated layer sequence on the fabric substrate.

Figure 2 (d) clearly shows that the flattened AgNW were covered by the ZnO-NP and successfully coated by the spray-deposition of a P3HT:ICBA active layer. The PEDOT:PSS layer was difficult to observe in the cross-section image, since it is relatively thin compared to the AgNW film. The P3HT:ICBA blend used in this study generally performs well with thicker films, unlike other high performance organic polymers that require an optimised thickness of around 100-200 nm. The J/V measurements of the solar cells studied in this work are shown in figures 3 and 4 and the results are summarised in table 1. Device type 1 was fabricated on the fabric and gave a maximum PCE of 0.01% with a FF of 0.24, V_{OC} of 0.55 V and J_{SC} of 0.11 mA/cm^2, as shown in table 1. For comparison, device type 2 was spray-coated with the same functional layers on a glass substrate, which gave a maximum PCE of 0.1% with a FF of 0.30, V_{OC} of 0.61 V and J_{SC} of 0.76 mA/cm^2. As displayed in figure 4, the J/V curve of device type 2 indicates a higher rectification, which suggests better diode behaviour due to the smoother surface of the P3HT:ICBA layer and uniform coverage of the PEDOT:PSS layer. V_{OC} and FF values of the spray-coated OSCs on both fabric and glass substrates are nearly identical, but the J_{SC} is lower for the fabric OSCs. This may be attributed to the peeling-off stage from the alumina tiles after fabrication. Bending caused by the peeling-off stage may generate micro-sized cracks on the conductive and other functional layers, which will increase the resistance across the junction to further reduce the J_{SC} current. Thus device type 1 leads to a higher series resistance compared to the glass counterpart in device type 2. However, it can be seen from the J/V measurement plots that the fabric solar cells did not suffer significantly from peeling-off from the alumina tiles, as shown in figure 3. The transmittance spectra of the fully solution processed organic solar cells and the AgNW films are displayed in figure 5 alongside a standard ITO electrode for reference. It can be seen that the spray-coated AgNW electrode (sheet resistance = 60 Ω/sq and T = 75% at 550 nm), shows high transmittance characteristics in the visible region of 450-850 nm. However, the AgNW electrode showed a lower transmittance than the ITO film, which is attributed to the increased AgNW density and improved contact of nanowires.

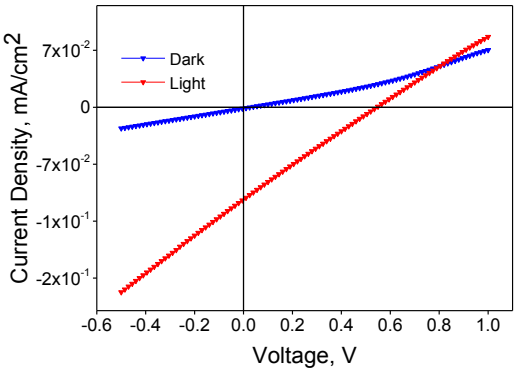

Fig. 3 J/V characteristics of OSCs fabricated on a fabric substrate using the spray-coating method represented as device type 1.

The spray-coated solar cells on glass substrate (device type 2) show a transparency of 47% at 550 nm wavelength. Additionally, device type 2 displayed 60% transparency at wavelengths beyond 650nm as the P3HT:ICBA layer is largely absorption free and these types of devices are highly favourable for optoelectronic applications such as power generating windows and tandem solar cell devices. As discussed above, the fabric solar cells did function with ZnO-NP and P3HT:ICBA thicknesses of ~4 µm, as shown in figure 6a (i). However, these thick layers can cause high resistance across the junction while cells are under operation and this is reflected in the low PCE value of 0.01%. Therefore, thinner ZnO-NP and P3HT:ICBA were targeted for the optimising stage. As shown in figure 6a (ii), the devices were fabricated with an optimised layer thickness down to hundreds of nm for all the functional layers. It was initially found, however, that the thin ZnO-NP and P3HT:ICBA films fill the scaffold structure of the AgNW but fail to sufficiently separate the top and bottom electrodes which leads to a short circuit.

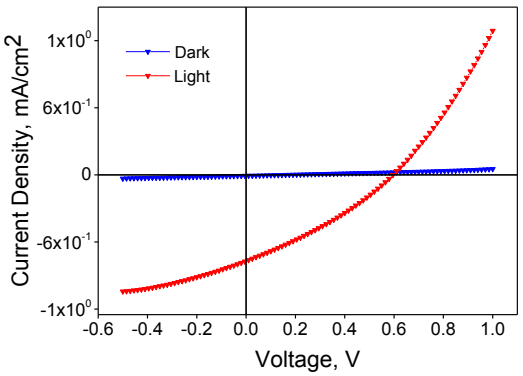

Fig: 4 J/V characteristics of OSCs fabricated on a glass substrate using the spray-coating method represented as device type 2.

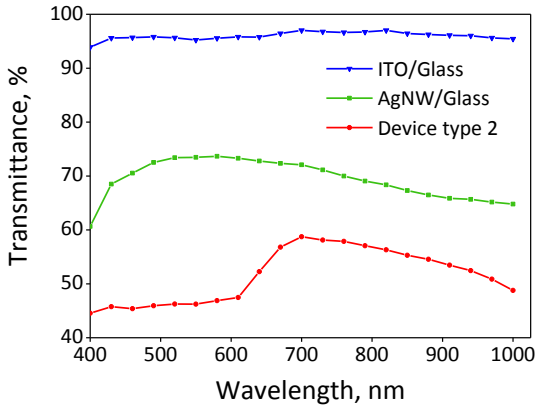

Fig. 5 Transmittance spectra of commercial ITO-coated glass, AgNW-coated glass and spray-coated semi-transparent solar cell device type 2.

In order to avoid a short circuit, the bottom AgNW layer was first flattened by compressing the nanowires while annealing the fabric devices at 150 °C for 15 minutes in an oven.[47, 53] The additional layers were then spray-coated giving the structure shown in figure 6a (iii). This approach prevented the short circuits and resulted in an increased photovoltaic performance (device type 3 in table 1). Device type 3 gave a maximum PCE of 0.02% with a FF of 0.25. Remarkably, after optimisation device type 3 demonstrated a two-fold increase of J_{SC} compared to device type 1. The cross-sectional SEM image of device type 3 in figure 6(b) clearly shows the individual layers with no interlayer mixing being observed even after greatly reducing the thickness of all the layers. From table 1, it should also be noted that the series resistance of device type 3 is less than a third of that found for device type 1. This may be due to interlayer mixing between the P3HT:ICBA/ZnO-NP and ZnO-NP/PEDOT:PSS layers which might have occurred in device type 1 but have been avoided in device type 3. Atomic force microscopic (AFM) measurements have been carried out on device type 3 to evaluate the surface morphology of each key functional layer in the deposited fabric solar cells. A 5µm × 5µm area of the films was scanned by the AFM in tapping mode. The surface roughness of the spray-coated AgNW on IF fabrics exhibited a root mean square (rms) value of 30 nm. The surface roughness of the spray-coated ZnO-NP on AgNW/IF fabrics increases as shown in figure 7. The image reveals that the surface roughness has increased with an rms value of 287 nm. Referring to figure 8, it can be seen that the P3HT:ICBA film smooths out the surface roughness of the ZnO-NP film. The P3HT:ICBA film contains nanocrystalline grains with an average diameter of about 60–80 nm and the resulting film roughness rms equals 44 nm.

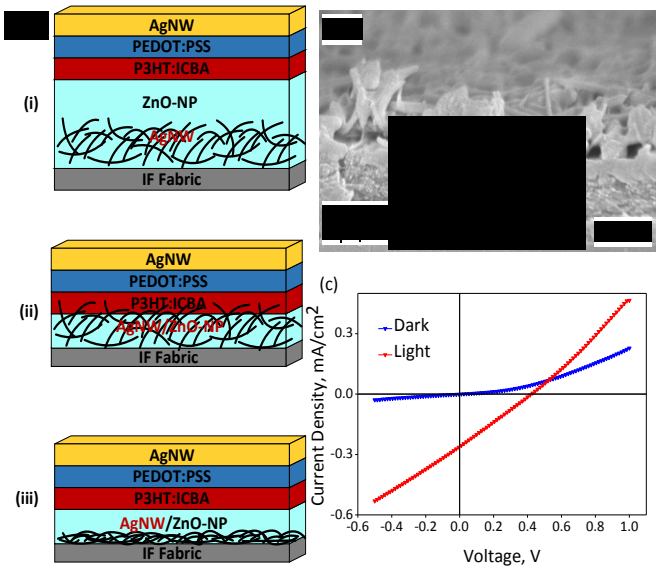

Fig. 6 (a) Cross-sectional view of the fabrication process for device optimisation in the staged approached sequence, (b) cross-sectional SEM image of the optimised functional layer thickness, (c) J/V characteristics of AgNW-pressed OSCs fabricated on a fabric substrate using the spray-coated method (device type 3).

Devices	Device configuration	V_{OC} (V)	FF	J_{SC} (mA/cm2)	PCE (%)	R_S (kΩ)	R_{SH} (kΩ)
Type 1	IF Fabric/AgNW/ZnO-NP/P3HT: ICBA/PEDOT:PSS/AgNW	0.55	0.24	0.11	0.01	83.7	76.7
Type 2	Glass/AgNW/ZnO-NP/P3HT: ICBA/PEDOT:PSS/AgNW	0.61	0.30	0.76	0.14	7.6	20.2
Type 3	IF Fabric/Pressed AgNW/ZnO-NP/P3HT: ICBA/PEDOT:PSS/AgNW	0.41	0.25	0.26	0.02	25.3	28.2

Table 1 Summary of the spray-coated solar cell characteristics on both fabric and glass substrates.

This level of surface roughness is not ideal and may lead to the recombination of holes and electrons and hence a reduced photocurrent. For comparison, we also fabricated OSCs using spin-coating and evaporation methods on fabric (device type 4) and glass substrates (device type 5). Device type 4 used evaporated aluminium as the bottom electrode followed by spin coated PEDOT:PSS and P3HT:ICBA layers. A semi-transparent top electrode was formed by evaporating 10nm of calcium and aluminium. Device type 4 gave a maximum PCE of 5×10^{-3}% with a FF of 0.26, a V_{OC} of 0.74 V and an J_{SC} of 0.02 mA/cm^2, as shown in table SI1. Device type 5 was fabricated with a conventional architecture of spin-coated PEDOT:PSS and P3HT:ICBA layers on an ITO glass substrate. The device was completed by thermal evaporation of 40nm of calcium and 40nm aluminium and gave a maximum PCE of 4.5% with a high fill factor of 0.63. The J/V curves of device types 4 and 5 are displayed in figure SI1. Considering the two fabric solar cells (3 and 4) made by different fabrication processes, device type 3 exhibited a higher PCE (0.02%) than device type 4 (5×10^{-3}%). The higher series resistance as shown in table SI1 may explain the reduced PCE in device type 4.

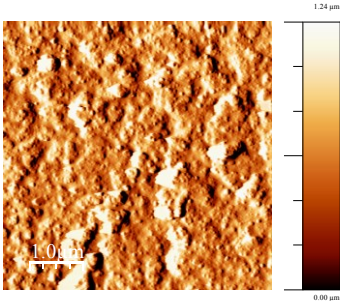

Fig. 7 AFM image of the spray-coated ZnO-NP layer on top of the spray-coated AgNW layer on the IF substrate.

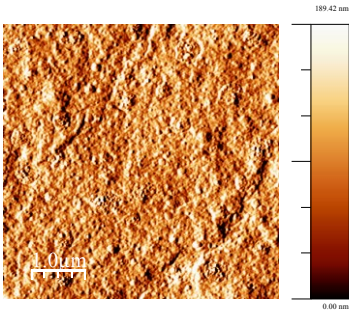

Fig. 8 AFM image of the spray-coated P3HT:ICBA layer on top of the ZnO-NP/AgNW layer on the IF substrate.

Further work will focus on optimising the thickness of the ZnO-NP and P3HT:ICBA layers in order to improve the collection of electrons from the device and to maximise light absorption respectively. Furthermore, a spray-coated encapsulation layer will be investigated in the future to protect the device and enhance its durability and lifetime. As this fully spray-coated organic solar cells on textiles substrate approach is targeting the wearable electronics industry in energy harvesting applications for powering on-body sensors and communications externally, the durability study is essential towards to later stage of this work. We have carried out the initial automotive bending test against the different radius (2.5 cm, 1 cm and 0.5 cm) of the bending rail in 100 and 200 cycles. The preliminary results show the performance of the fabrics solar cells have lost their photonic functionalities. The main issues we identified for the cause of failure are due to additional materials added for the purposes of testing and protecting the devices. Electrical connection to the electrodes on each device was achieved using a silver epoxy dot for testing purposes. This is a stiff material and during bending damaged the functional layers and cell structure. In addition, for the purposes of the cyclical bending test the cells are placed in pocket in a stretchable textile band and to prevent this from rubbing the layers, a protective UV curable epoxy encapsulation layer was added. However, this was found to be too rigid and caused the device layers to delaminate from the textile substrate destroying the cell structure. However, the encapsulation material was evaluated on the spray coated solar cells on glass substrates in order to determine if they do successfully seal the cells with degrading performance. Cells were fabricated on glass and their efficiency tested immediately after fabrication but before encapsulation. The cells were then encapsulated and tested again and the PCE was found to be unaffected by the encapsulations process. The encapsulation layer was also found to protect the cells against oxidation with encapsulated cells demonstrating performance of 0.1% PCE straight after fabrication and after 4 days stored in ambient atmosphere. Un-encapsulated cells were completely non-functional after 4 days storage in ambient atmosphere. In order to test the robustness of the functional layers flexible electrical and encapsulating layers have to be used that can themselves withstand the bending test. We are currently reviewing and investigating of highly flexible encapsulation transparent layers that minimise the strain force developed in the functional layers during the bending test. Similarly, flexible conductive materials are under investigation and this research

is ongoing in order to improve the durability of the fabric solar cells.

Conclusions

In summary, fully spray-coated fabric solar cells on standard polyester cotton fabrics have been demonstrated. The standard polyester cotton fabric was pre-treated with a screen printed interface layer to significantly reduce surface roughness and obtain compatible wettability for the subsequent deposition of functional inks. The results gave a maximum PCE of 0.01% for all the solution-processed spray-coated fabric solar cells and 5 × 10^{-3}% for spin-coated fabric solar cells. The optimised spray-coated solar cells on fabric substrates gave a maximum PCE of 0.02% when the thickness of the ZnO-NP and P3HT:ICBA layers were reduced. Compressing the bottom AgNW layer during the annealing stage prevents short circuits and lowered the resistance, whilst reducing the thickness of the ZnO-NP layer in the optimised device also improved device performance. An optimised solution may be used to manufacture energy harvesting textiles to integrate into and supply the power source to wearable electronics systems.

Acknowledgements

This work was supported by Sensor Platform for HEalthcare in a Residential Environment (SPHERE) project (EP/K031910/1). Professor S. P. Beeby acknowledges EPSRC support through his Fellowship 'Energy Harvesting Materials for Smart Fabrics and Interactive Textiles' (EP/I005323/1). Professor P. J. Skabara thanks the Royal Society for a Wolfson Research Merit Award. All data supporting this study are openly available from the University of Southampton repository at http://dx.doi.org/10.5258/SOTON/376690

References

1. M. A. Green, K. Emery, Y. Hishikawa, W. Warta and E. D. Dunlop, *Prog. Photovoltaics Res. Appl.*, 2014, **22**, 701-710.
2. F. Dimroth, M. Grave, P. Beutel, U. Fiedeler, C. Karcher, T. N. D. Tibbits, E. Oliva, G. Siefer, M. Schachtner, A. Wekkeli, A. W. Bett, R. Krause, M. Piccin, N. Blanc, C. Drazek, E. Guiot, B. Ghyselen, T. Salvetat, A. Tauzin, T. Signamarcheix, A. Dobrich, T. Hannappel and K. Schwarzburg, *Prog. Photovoltaics Res. Appl.*, 2014, **22**, 277-282.
3. H. M. Upadhyaya, S. Senthilarasu, M.-H. Hsu and D. K. Kumar, *Sol. Energy Mater. Sol. Cells*, 2013, **119**, 291-295.
4. S. Senthilarasu, E. F. Fernandez, F. Almonacid and T. K. Mallick, *Sol. Energy Mater. Sol. Cells*, 2015, **133**, 92-98.
5. J. Yan and B. R. Saunders, *RSC Advances*, 2014, **4**, 43286-43314.
6. J. Peet, M. L. Senatore, A. J. Heeger and G. C. Bazan, *Adv. Mater.*, 2009, **21**, 1521-1527.
7. C. J. Brabec, N. S. Sariciftci and J. C. Hummelen, *Adv. Funct. Mater.*, 2001, **11**, 15-26.
8. S. Günes, H. Neugebauer and N. S. Sariciftci, *Chem. Rev.*, 2007, **107**, 1324-1338.
9. A. C. Matteo Stoppa, *Sensors*, 2014, **14**, 11957-11992.
10. K. Yang, C. Freeman, R. Torah, S. Beeby and J. Tudor, *Sensors and Actuators A: Physical*, 2014, **213**, 108-115.
11. C. Hertleer, H. Rogier, L. Vallozzi and L. Van Langenhove, *Antennas and Propagation, IEEE Transactions on*, 2009, **57**, 919-925.
12. R. J. N. Helmer, M. A. Mestrovic, D. Farrow, S. Lucas and W. Spratford, *Adv. Sci. Tech.*, 2008, **60** 144-153
13. M. B. Schubert and J. H. Werner, *Mater. Today*, 2006, **9**, 42-50.
14. H. Sun, X. You, J. Deng, X. Chen, Z. Yang, P. Chen, X. Fang and H. Peng, *Angew. Chem. Int. Ed.*, 2014, **53**, 6664-6668.
15. X. Fang, Z. Yang, L. Qiu, H. Sun, S. Pan, J. Deng, Y. Luo and H. Peng, *Adv. Mater.*, 2014, **26**, 1694-1698.
16. S. Pan, Z. Yang, H. Li, L. Qiu, H. Sun and H. Peng, *J. Am. Chem. Soc.*, 2013, **135**, 10622-10625.
17. T. Chen, L. Qiu, Z. Cai, F. Gong, Z. Yang, Z. Wang and H. Peng, *Nano Lett.*, 2012, **12**, 2568-2572.
18. Z. Yang, H. Sun, T. Chen, L. Qiu, Y. Luo and H. Peng, *Angew. Chem. Int. Ed.*, 2013, **52**, 7545-7548.
19. Z. Yang, J. Deng, X. Sun, H. Li and H. Peng, *Adv. Mater.*, 2014, **26**, 2643-2647.
20. S. Pan, Z. Yang, P. Chen, J. Deng, H. Li and H. Peng, *Angew. Chem. Int. Ed.*, 2014, **53**, 6110-6114.
21. Z. Zhang, X. Chen, P. Chen, G. Guan, L. Qiu, H. Lin, Z. Yang, W. Bai, Y. Luo and H. Peng, *Adv. Mater.*, 2014, **26**, 466-470.
22. H. Sun, X. You, J. Deng, X. Chen, Z. Yang, J. Ren and H. Peng, *Adv. Mater.*, 2014, **26**, 2868-2873.
23. T. Chen, L. Qiu, Z. Yang, Z. Cai, J. Ren, H. Li, H. Lin, X. Sun and H. Peng, *Angew. Chem. Int. Ed.*, 2012, **51**, 11977-11980.
24. T. Chen, S. Wang, Z. Yang, Q. Feng, X. Sun, L. Li, Z.-S. Wang and H. Peng, *Angew. Chem. Int. Ed.*, 2011, **50**, 1815-1819.
25. L. Li, Z. Yang, H. Gao, H. Zhang, J. Ren, X. Sun, T. Chen, H. G. Kia and H. Peng, *Adv. Mater.*, 2011, **23**, 3730-3735.
26. A. A. Arbab, K. C. Sun, I. A. Sahito, M. B. Qadir and S. H. Jeong, *PCCP*, 2015, **17**, 12957-12969.
27. J. Xu, M. Li, L. Wu, Y. Sun, L. Zhu, S. Gu, L. Liu, Z. Bai, D. Fang and W. Xu, *J. Power Sources*, 2014, **257**, 230-236.
28. I. A. Sahito, K. C. Sun, A. A. Arbab, M. B. Qadir and S. H. Jeong, *Electrochim. Acta*, 2015, **173**, 164-171.
29. A. Bedeloglu, A. Demir, Y. Bozkurt and N. S. Sariciftci, *Synth. Met.*, 2009, **159**, 2043-2048.
30. A. Bedeloglu, R. Koeppe, A. Demir, Y. Bozkurt and N. Sariciftci, *Fibers and Polymers*, 2010, **11**, 378-383.
31. A. Bedeloglu, P. Jimenez, A. Demir, Y. Bozkurt, W. K. Maser and N. S. Sariciftci, *The Journal of The Textile Institute*, 2011, **102**, 857-862.
32. A. Bedeloglu, A. Demir, Y. Bozkurt and N. S. Sariciftci, *Renewable Energy*, 2010, **35**, 2301-2306.
33. F. C. Krebs, M. Biancardo, B. Winther-Jensen, H. Spanggard and J. Alstrup, *Sol. Energy Mater. Sol. Cells*, 2006, **90**, 1058-1067.
34. S. Lee, Y. Lee, J. Park and D. Choi, *Nano Energy*, 2014, **9**, 88-93.
35. D. Zou, Z. Lv, X. Cai and S. Hou, *Nano Energy*, 2012, **1**, 273-281.
36. B. O'Connor, K. P. Pipe and M. Shtein, *Appl. Phys. Lett.*, 2008, **92**, 193306.

37. A. Bedeloglu, A. Demir, Y. Bozkurt and N. S. Sariciftci, *Textile Research Journal*, 2010, **80**, 1065-1074.
38. J. W. Liu, M. A. G. Namboothiry and D. L. Carroll, *Appl. Phys. Lett.*, 2007, **90**, 063501.
39. http://www.powerweave.eu/index.php/public-documents/posters.
40. R. R. M. J. I. B. Wilson, H. Lind and A.G. Diyaf, *Modern Energy Review*, 2012, **4**, 68-69.
41. K. Norrman, A. Ghanbari-Siahkali and N. B. Larsen, *Annual Reports Section "C" (Physical Chemistry)*, 2005, **101**, 174-201.
42. C. Girotto, B. P. Rand, J. Genoe and P. Heremans, *Sol. Energy Mater. Sol. Cells*, 2009, **93**, 454-458.
43. P. Kopola, T. Aernouts, R. Sliz, S. Guillerez, M. Ylikunnari, D. Cheyns, M. Valimaki, M. Tuomikoski, J. Hast, G. Jabbour, R. Myllyla and A. Maaninen, *Sol. Energy Mater. Sol. Cells*, 2011, **95**, 1344-1347.
44. T. Imai, N. Shibayama, S. Takamatsu, K. Shiraishi, K. Marumoto and T. Itoh, *Jpn J Appl Phys*, 2013, **52**.
45. T. Imai, S. Takamatsu, K. Shiraishi, K. Marumoto and T. Itoh, *Procedia Engineering*, 2012, **47**, 502-505.
46. J. Krantz, M. Richter, S. Spallek, E. Spiecker and C. J. Brabec, *Adv. Funct. Mater.*, 2011, **21**, 4784-4787.
47. D. S. Leem, A. Edwards, M. Faist, J. Nelson, D. D. C. Bradley and J. C. de Mello, *Adv. Mater.*, 2011, **23**, 4371-4375.
48. T. Stubhan, J. Krantz, N. Li, F. Guo, I. Litzov, M. Steidl, M. Richter, G. J. Matt and C. J. Brabec, *Sol. Energy Mater. Sol. Cells*, 2012, **107**, 248-251.
49. M. Song, J. Park, C. Kim, D. H. Kim, Y. C. Kang, S. H. Jin, W. Y. Jin and J. W. Kang, *Nano Research*, 2014, **7**, 1370-1379.
50. F. Guo, P. Kubis, T. Stubhan, N. Li, D. Baran, T. Przybilla, E. Spiecker, K. Forberich and C. J. Brabec, *ACS Appl. Mater. Interfaces*, 2014, **6**, 18251-18257.
51. F. Guo, X. Zhu, K. Forberich, J. Krantz, T. Stubhan, M. Salinas, M. Halik, S. Spallek, B. Butz, E. Spiecker, T. Ameri, N. Li, P. Kubis, D. M. Guldi, G. J. Matt and C. J. Brabec, *Adv. Energy Mater.*, 2013, **3**, 1062-1067.
52. S. B. Kang, Y. J. Noh, S. I. Na and H. K. Kim, *Sol. Energy Mater. Sol. Cells*, 2014, **122**, 152-157.
53. J. Ajuria, I. Ugarte, W. Cambarau, I. Etxebarria, R. Tena-Zaera and R. Pacios, *Sol. Energy Mater. Sol. Cells*, 2012, **102**, 148-152.